European Journal of Chemistry

View Journal Online
View Article Online

Theoretical study of a single-walled carbon nanotube and a cellulose biofiber as 5-fluorouracil anti-cancer drug carriers

Eshraq Ahmed Abdullah *

Department of Chemistry, Faculty of Education, Taiz University, Taiz, 009674, Yemen

* *Corresponding author at: Department of Chemistry, Faculty of Education, Taiz University, Taiz, 009674, Yemen.*
e-mail: ali123456yemen@gmail.com (E.A. Abdullah).

RESEARCH ARTICLE

10.5155/eurjchem.13.1.69-77.2188

Received: 26 September 2021
Received in revised form: 22 November 2021
Accepted: 23 November 2021
Published online: 31 March 2022
Printed: 31 March 2022

KEYWORDS

Adsorption
Drug delivery
5-Fluorouracil
DMol3 module
Cellulose biofiber
Single walled carbon nanotube

ABSTRACT

Chemotherapy is one of the most valuable and widely available option in cancer treatment. However, a method of delivering the drug to achieve a therapeutic effect still a considerable challenge. Therefore, this study seeks to identify the non-bonding interaction of 5-fluorouracil anticancer drug with a single walled carbon nanotube and a Cellulose bio-fiber using density functional theory and molecular mechanics simulations. To do that, adsorption locator and DMol3 modules were utilized to determine the electronic and optical properties of carriers before and after adsorption processes. The interaction energies indicate that the 5-fluorouracil molecule can physically adsorb and the optimized geometries are stable. The charge transfer occurs between N4-H10 bond of the 5-fluorouracil molecule and the cellulose carrier by a synergistic effect of hydrogen bond formation and van der Waals forces. This effect smoothly transforms into van der Waals interactions by O3, N4, and N5 atoms in the case of single-walled carbon nanotubes. There is a clear difference in the absorption peak and a significant narrowing of the molecular energy gap of a cellulose complex because of the shifting of the electron accepting center to a drug molecule. The conductor-like screening model shows the affinity of the complexes toward hydrogen bond acceptor, which enhances their solubility in biological systems. A remarkable influence in the case of the cellulose complex works as a starting point to use natural polymers as drug delivery carriers.

Cite this: *Eur. J. Chem.* **2022**, *13(1)*, 69-77 **Journal website**: www.eurjchem.com

1. Introduction

Cancer disease ranks as the second cause of death in the world today [1]. In this regard, doctors employ many types of drugs to slow tumor growth and cure cancer. Among them, a 5-fluorouracil molecule (5-FU) is still an interesting drug in pharmacology to remedy the cancer of lung, colon, skin, stomach, gastrointestinal, and breast [2]. The inhibition role of the 5-FU drug during nucleoside metabolism of thymidylate synthetase enzyme prevents the conversion of deoxyuridylic acid to thymidylic acid. This process can significantly decrease a cell cytotoxicity and slow tumor growth [3,4]. However, a very short biological half-life, a lower duration of drug retention in tumors, and drug resistance limits its clinical use [5]. In order to surmount these disadvantages, researches in both computational and experimental studies have focused their efforts to deliver a drug in a biological system using different type of carriers [6].

In the modern era of technology, nanomaterials such as Nanotubes considered the most attractive nano-carriers due their ability to cross the cell membrane, special physico-chemical properties such as; a large surface area, a low toxicity, a low weight and their surface functionalization ability [7]. Therefore, the incorporation of a biological active molecule inside the nanocarrier not just protects the drug molecule from the degradation process, but also overcomes the mechanical, physicochemical, and the enzymatic resistance of the biological barriers [8].

The same possibility also observed using natural bio-fiber polymers such as Cellulose due to their less toxicity, high drug loading and encapsulation efficiency [9,10]. However, how does the interaction occur between Nano carrier and the 5-FU anticancer drug? How do the characters of the 5-FU drug can bring different effects on carrier properties, still a big challenge in the literature?

Previous studies have indicated that 5-FU could bind to nanostructures carrier through physical and/or chemical interactions making complex systems. Khoshbayan *et al.* showed that the 5-FU molecule could attach to nanoparticles through N, O, F, C, and H atoms of the pyrimidine ring, which work as adsorption links on a possible drug delivery process [11]. In another effort, Kurban and Muz clarified that the 5-FU drug can use oxygen atoms of a pyrimidine ring as adsorption sites for interaction with doped carbon nanotube carriers [12]. In another study, the 5-FU drug molecule showed its ability to use carbonyl groups to make a doubly hydrogen bond with the graphene oxide nanosheet edge, in which O···H bond with donor-acceptor distances of 2.610 to 2.949 Å [4].

https://dx.doi.org/10.5155/eurjchem.13.1.69-77.2188

Table 1. The adsorption energy values for the most stable configurations.

Energy (E) Kcal/mol	E_{Total}	$E_{Adsorption}$	$E_{Rigid\ adsorption}$	$E_{Deformation}$	dE_{ad}/dNi
5-FU/SWCNT	-0.69	-9.86	-9.88	0.02	-9.86
5-FU/Cellulose	-0.16	-9.33	-9.34	0.01	-9.33

The covalently linkage between a carrier surface and a nitrogen head was observed in Javan *et al.* study, when he utilized $B_{12}N_{12}$ nanocage as a drug delivery device for the free and tautomeric forms of the 5-FU drug [13]. Wazzan *et al.* explained that a chemisorption behavior between 5-FU drug and gallium nitride is due to the relocation of one Hydrogen atom, which belongs to N-H bond of the 5-FU ring to the nearest gallium nitride atoms [14]. In this context, this study aims to understand the adsorption behaviors of the 5-FU drug on an armchair single-walled carbon nanotube (SWCNT) and a molecular bio-fiber cellulose, which recently utilize as carriers for in vivo drug delivery. To do that, the (6,6) SWCNT with the stoichiometry of $C_{24}H_{24}$ was selected as a model of a first carrier, whereas the molecular cellulose biofiber with the stoichiometry of $C_{18}H_{32}O_{16}$ was shown as a second one in the initial step. Then, a Monte Carlo (MC) simulation was carried out to determine the adsor-ption minimum energy and to study the interaction behavior of the drug attached to a carrier. In final step, the optical properties, density of states around molecular band gaps, and a solvent effect of the 5-FU anticancer drug, carriers and the considered complexes were analyzed using ab initio density functional theory (DFT) to give a clear picture of the interaction natural. To the best of our knowledge, no available literature had ever made a comparative study of SWCNT and the molecular Cellulose as potential 5-FU drug delivery carriers.

2. Computational methods

The non-bonded interaction between SWCNT in which its end atoms saturated with hydrogen atoms to reduce the boundary effects, and cellulose as a bio-fiber resource with an anticancer drug 5-FU in the solvent water was theoretical simulated. In detail, adsorbate, carrier and their complexes were initially optimized using Universal Forcite Field (UFF) executed in the BIOVIA Material studio software [15] using a smart algorithm. Geometries were converged when a gradient of 1.0×10^{-3} kcal/mol was achieved. The truncation method was a cubic spline with the cutoff distance of 12.0 Å. Molecular mechanics (MM) uses the classical physics to describe a molecule in terms of its internal coordinates, which makes Forcite module an advanced tool for quick and trustable configuration search. Therefore, in a second step, an adsorption locator module utilizes a Monte Carlo (MC) searching to find out low energy adsorption sites on a carrier according to Boltzmann probabilities [16]. To clarify the impact of the adsorption process, DMol3 simulation was finally used to elucidate the important features of the optimized 5-FU adsorbate before putting on the carrier, isolated carriers and their stable adsorption configurations [17,18]. In more detail, an orbital overlapping density of states (DOS) and molecular orbital (HOMO-LUMO) properties are acquired using the exchange and correlation scheme of Perde-Burke-Emzerhof functional with a generalized gradient (GGA/PBE) approxi-mation. To describe the solvent and solute performance with respect to polar interactions, the sigma profiles of study systems were generated using the Conductor like Screening Model (COSMO), which helps to identify hydrogen bond donor (HBD) and hydrogen bond acceptor (HBA) regions.

3. Results and discussion

The theoretical results have been obtained by two methods. The first method involves a molecular mechanics simulation that was used to select the most stable configurations of adsorption. While in second method, quantum mechanics were carried out to describe the important features of the selected configurations. Thus, it is useful to use the same sequence to discuss the results in the following sections.

3.1. Adsorption locator studies

Adsorption locator assists to find the energetically stable sites for adsorption using Equation (1):

$$E_{\text{Adsorption}} = E_{\text{Rigid adsorption}} + E_{\text{Deformation}} \quad (1)$$

where $E_{\text{Adsorption}}$ is the adsorption energy releases when the relaxed 5-FU drug molecule was adsorbed on the carrier surface, $E_{\text{Rigid adsorption}}$ is the energy released or required, when the unrelaxed 5-FU drug molecule was adsorbed on the carrier surface, i.e., before the geometry optimization step. $E_{\text{Deformation}}$ is the energy released or required, when the 5-FU drug molecule was relaxed on the carrier surface, i.e., after the geometry optimization step. The adsorption energy values for the most stable configurations are outlined in Table 1, which also gives the total energy of adsorption as the sum of the internal and adsorption energies and dE_{ad}/dNi, which refers to the energy of the 5-FU/carrier complexes when one of the 5-FU drug has been removed.

The adsorption energies were estimated to be -9.86 and -9.33 kcal/mol for 5-FU/SWCNT and 5-FU/Cellulose complexes, respectively. A negative value indicates that the drug can spontaneously adsorb on a carrier surface and the process is thermodynamically favorable [19]. The dE_{ad}/dNi values for the two carriers are quite similar, which may indicate the similarity of the interaction forces involved in the adsorption. These types of intermolecular forces can easily be observed in Figure 1.

Figure 1 demonstrates that the intramolecular energy is the dominant adsorption energy for both complexes followed by weak van der Waals energy. The intramolecular energy for adsorption increases up to 9.17 kcal/mol for both complexes. However, the average total energy extracted from the last step of a Monte Carlo simulation shows an increase of the average total energy of 3.65 kcal/mol for the 5-FU/Cellulose complex compared to 2.52 kcal/mol for the 5-FU/SWCNT complex. This higher average total energy can be attributed to the different structural characteristics of drug/carrier complex. As shown in Figure 2, the 5-FU molecule is located inside the SWCNT tube through the O3, N4, and N5 atoms due to their electro-negatively centers. These adsorption sites have been noticed separately in the previous literature [12]. In case of the 5-FU/Cellulose complex, the 5-FU ring is located over the cellulose carrier, in which the N4-H10 bond of the 5-FU ring works as the nearest center of interaction.

3.2. DMol3 study

3.2.1. Structure and electronic properties

To clarify the impact of 5-FU delivery on selected carriers, the energetically favorable UFF configuration candidate was subjected to further optimized by ab initio Density functional theory using DMol3 module implemented in a Material studio package at the GGA/PBE level of theory. The optimization step was done in a water solvent, which has a dielectric constant of 78.4 in order to mimic the human biological system.

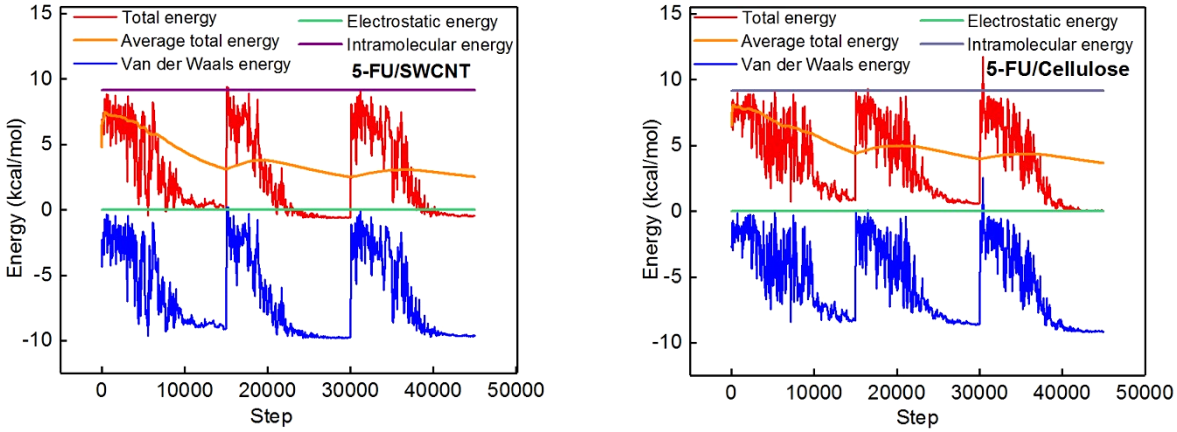

(a) **5-FU/SWCNT** (b) **5-FU/Cellulose**

Figure 1. The interaction forces involved in the adsorption.

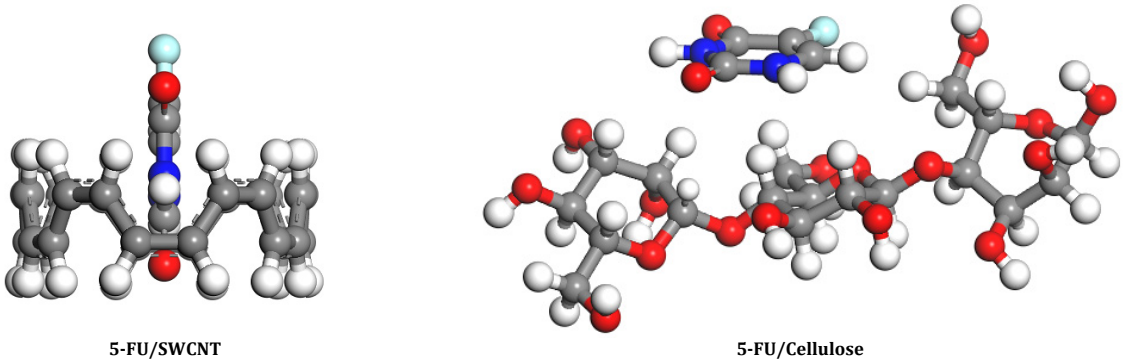

5-FU/SWCNT **5-FU/Cellulose**

Figure 2. The structural characteristic of the most stable configuration drug/carrier complex on an adsorption locator module.

The optimized geometries of the 5-FU/SWCNT and the 5-FU/Cellulose complexes within the minimum intermolecular distance between the most active adsorption sites are depicted in Figure 3.

The shortest contact distances recorded between these groups and the nearest hydrogen atoms of the SWCNT tube are 3.46, 3.63, and 3.52 Å, respectively. This interaction range shows that the SWCNT and 5-FU do not chemically interact with each other, but have a physical adsorption-like bonding. For the 5-FU/Cellulose complex, the close contact distances are 2.434 and 2.540 Å for the 5-FU C-N4···H44 and the 5-FU N4-H10···O10 Cellulose hydrogen bonds, respectively. These close contacts still less than the values of a doubly hydrogen bond formed between the carbonyl group of the 5-FU drug at the edge of Graphene Oxide Nanosheet [4]. Boraei *et al.* also showed that pyran-2,4-diones molecules could be packed in their crystals via N-H···O hydrogen bonding interactions with donor-acceptor distances of 2.991 Å [20]. However, there are no clear limits to the A-H···B hydrogen bond distance in the literature, where A and B are center atoms linked to the hydrogen. Grabowski (2021) showed that the Strong H-bonds interaction takes a range of 2.7-3.0 Å, while the weak H-bond interaction takes a range of 3.0-3.5 Å. This bond can easily transform into the van der Waals interaction if the distance increases up to 3 Å [21]. Based on this classification, the interaction the 5-FU/SWCNT complex is mainly governed via van der Waals, and there is a probability of hydrogen bond formation in the case of the 5-FU/Cellulose complex. This finding implies that, the adsorption of the 5-FU can transform the structure, electronic properties of the Cellulose carrier using complex types of interactions. Our results in agreement with Company *et al.* who showed an existence of a cooperation behavior between H-bonding and usual dispersion forces during the 5-FU adsorption over hydrated silica [22].

3.2.2. Binding energy

The binding energy (E_{Binding}) between a 5-FU drug and carrier is evaluated by Equation (2):

$$E_{binding} = E_{5-FU/carrier} - (E_{carrier} + E_{5-FU}) \quad (2)$$

where $E_{\text{5-FU/carrier}}$ is the total electronic energy of 5-FU loaded on a carrier, the E_{carrier} and $E_{\text{5-FU}}$ are the individual electronic energies of pure carrier and 5-FU drug, respectively, after DMol3 geometry optimization [23]. The binding energy of the 5-FU/Cellulose complex is -11.56 kcal/mol. This energy negatively shits to -18.27 kcal/mol in the case of the 5-FU/SWCNT complex. The negative values of the energy mean that the more energy is required to disassemble any complex, and the 5-FU/SWCNT complex has a greater stability.

3.3. Molecular orbital analysis

Figure 4 illustrates the lowest unoccupied molecular orbital (LUMO) and the highest occupied molecular orbital (HOMO) of the pure substances, 5-FU/SWCNT and 5-FU/Cellulose complexes. It is clearly observable that the HOMO and LUMO orbitals are localized over the axis of a nanotube, where the most contribution is coming from carbon atoms. The HOMO and LUMO orbitals of the 5-FU are generally localized over the whole molecule except for the N-H bond that shows anti-bonding character in HOMO orbitals.

Table 2. The molecular band edge positions, band gap (E_{gap}) and their chemical potentials of studied systems.

Parameter eV)	5-FU	SWCNT	5-FU/SWCNT	Cellulose	5-FU/Cellulose
E_{HOMO}	-5.804	-4.302	-4.450	-5.855	-5.835
E_{LUMO}	-2.078	-2.679	-2.610	0.390	-2.228
E_{gap}	3.726	1.623	1.840	6.245	3.607
μ	3.941	3.491	3.530	2.733	4.032

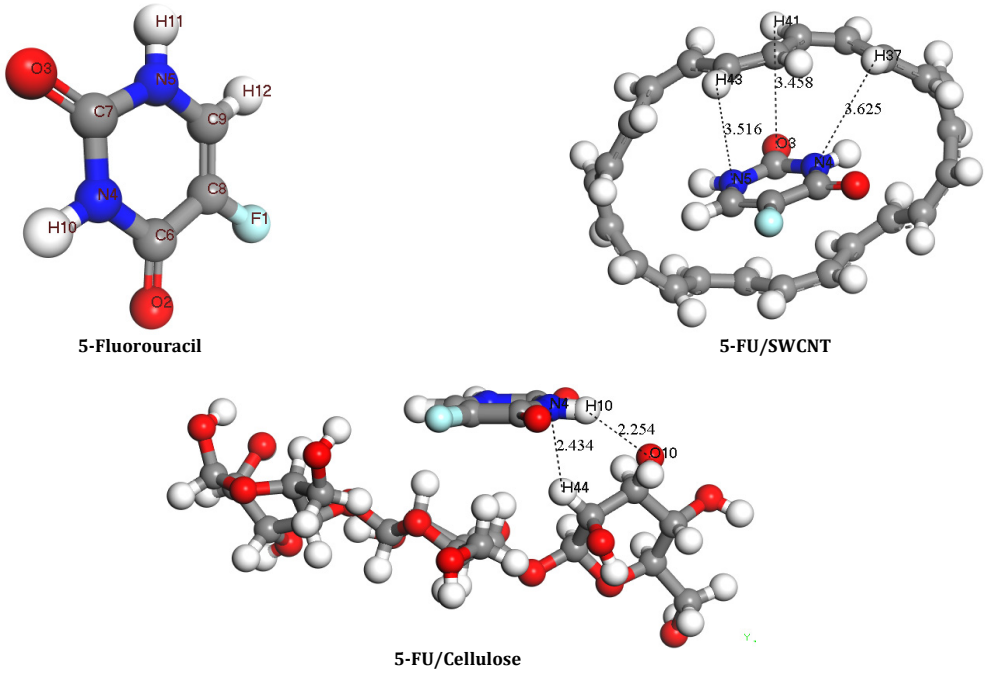

Figure 3. The DMol3 optimized geometries of the 5-FU/SWCNT and 5-FU/Cellulose complexes within the minimum intermolecular distance between the most active sits.

The bonding character over one keto carbonyl group was observed in LUMO orbitals. These results are in a good accordance with Khanmohammadi and Mohammadi, who investigated the effect of various solvents on 5-fluorouracil-vitamin B3 complex interaction using the Polarized Continuum Model [24]. In case of the Cellulose carrier, the HOMO orbitals are distributed to the functional groups of a cellobiose unit in the area around a β-glycosidic bond, which act as centers for the donation of electrons to the empty orbitals located at the equatorial hydroxyl group. The LUMO energy value of 0.390 eV indicates that the Cellulose carrier can play the role of an electron donor to form hydrogen bonds with N-H orbitals of the 5-FU drug.

The donating and accepting orbitals and interaction behavior upon adsorption are mostly governed by the energies of the molecular band edge positions of a drug/carrier complex. The molecular band edge positions, band gap (E_{gap}) and their chemical potentials, which are calculated by the Equations (3 and 4) [25] are shown in Table 2.

$$E_{gap} = (E_{LUMO} - E_{HOMO}) \quad (3)$$

$$\mu = -\left(\frac{E_{HOMO}+E_{LUMO}}{2}\right) \quad (4)$$

As can be seen in Table 2, the frontier orbital energy values of the 5-FU/SWCNT complex are similar to that of pure carrier, which reflects the ability of the complex to reproduce the charge transfer of the SWCNT carrier. The HOMO and LUMO orbitals are mainly located in a carrier. This evidently indicates that the HOMO and LUMO distributions of the 5-FU drug completely shift to a carrier during the adsorption. The drug loses its reactivity. Thus, SWCNT can act as a proper carrier for the delivery of 5-FU drug. This agrees well with Mirali *et al.* finding [26]. In the case of the 5-FU/Cellulose complex, the E_{HOMO} value is very similar to that of both pure 5-FU drug and the cellulose carrier.

However, the center of donation is only localized on the functional groups of a cellobiose unit, which implies the ability of a complex to reproduce the charge transfer of a carrier. Differently, LUMO energy value (E_{LUMO}) shifts from 0.390 eV in pure Cellulose to -2.228 eV in the complex, leading to an obvious decrease in the HOMO → LUMO gap of 3.607 eV.

This negative shift can be ascribed to the transfer of electron acceptation center from equatorial hydroxyl groups of the Cellulose carrier to the 5-FU ring during the adsorption process as shown in Figure 4. That is a forward donation from the Cellulose carrier to the 5-FU drug is a main ingredient of the chemical bonding. The 5-FU/Cellulose may produce a semi-conductor-like material. A lower value of frontier orbital gap also indicates that the 5-FU/Cellulose complex became more reactive to add an electron to the LUMO level and hence is more polarizable and chemically softer. However, the negative values of HOMO and LUMO levels reflect neither adding nor removing an electron may occur. These results elucidate that the electronic properties of the SWCNT carrier were preserved. Whereas the cellulose carrier became more sensitive to detect the drug and was converted to soft species upon adsorption.

3.4. Optical properties

Time dependent density function theory (TDDFT) calculations implemented in DMol3 module at GGA/PBE level of theory were used to investigate whether the interaction between the 5-FU drug and the carrier will produce a significant difference in their optical properties.

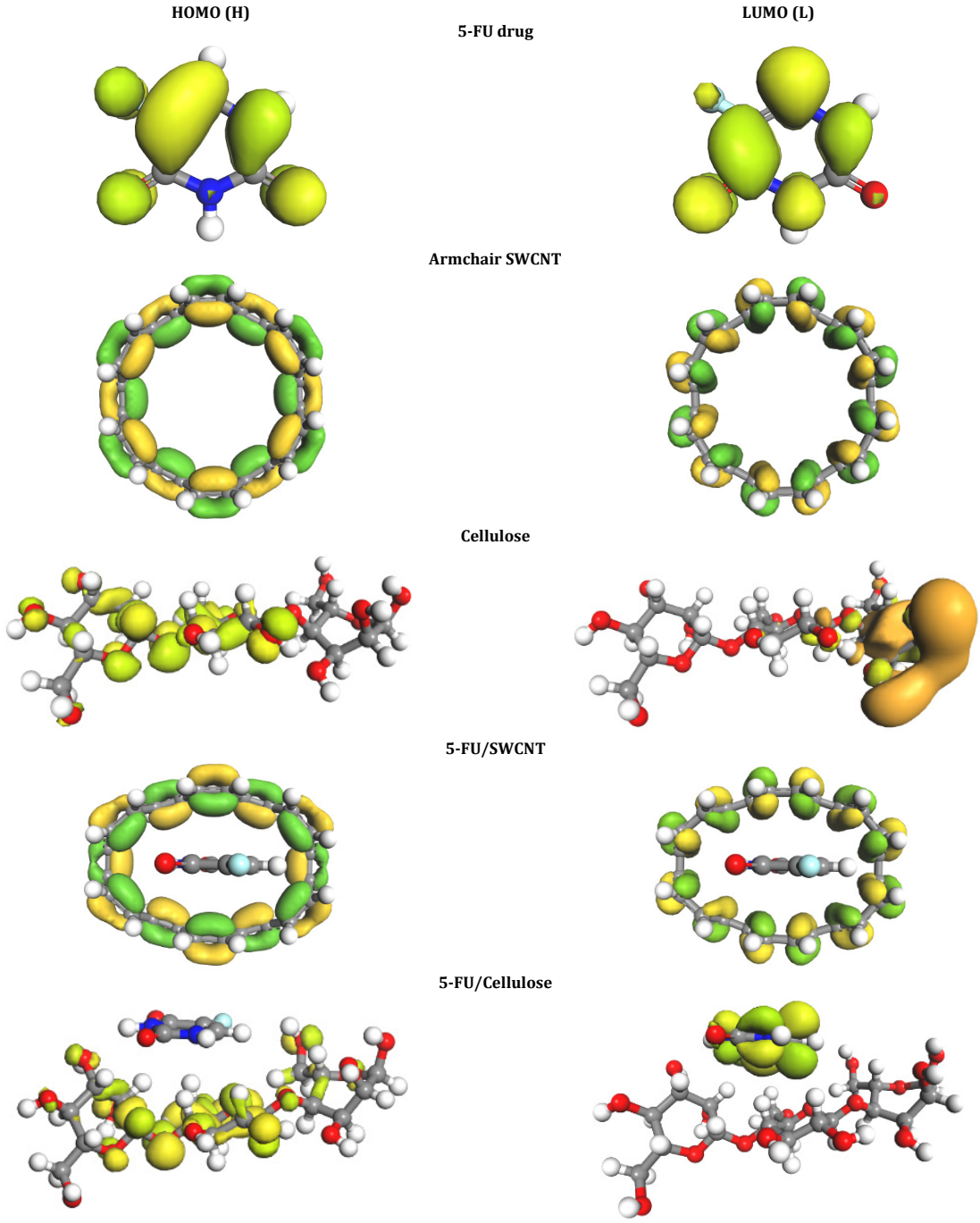

Figure 4. The HOMO (H) and LUMO (L) isosurfaces of the 5-FU drug, pure carrier and their complexes.

As could be seen in Figure 5, the 5-FU anticancer drug has one strong absorption peak at 171 nm and three very weak peaks at 144, 212, and 272 nm with oscillator strengths of 0.224, 0.155, 0.086, and 0.073, respectively. Theses charge transfer has been noticed from relative orbital contributions of H−1 → L+2, H−1 → L+4, H → L+1 and H → L, respectively. The absorption peak at a wavelength of 272 nm agrees well with the main peak of 266 nm obtained in the experimental spectrum recorded in Yusefi *et al.* study. This quantitative agreement implies a good simulation results at molecular edge positions [10]. In the case of SWCNT, the calculated absorption peaks have been observed at 287 and 406 nm with oscillator strengths of 0.734 and 0.782, respectively. These charge transfer can be ascribed to H−3 → L+1 and H−2 → L, respectively. The interaction between 5-FU drug and SWCNT carrier can only reproduce the second absorption peak of SWCNT at 408 nm. For the first absorption peak, a 26 nm red shift has been observed in case of the complex. Additionally, there is a clear decrease in peak intensity. This decrease is due to hypochromic effects arising from the π−π-stacking interaction of the 5-FU pyrimidine ring to the tube surface in agreement with Karachevtsev *et al.* finding, who attributed the attenuation of the UV-Vis light absorption of the SWCNT tube to the presence of pyrimidine oligonucleotide in DNA structure [27]. The Cellulose spectrum has one considerable absorption peak at a wavelength of 185 nm arising from charge transfer between H−3 → L+1 orbital.

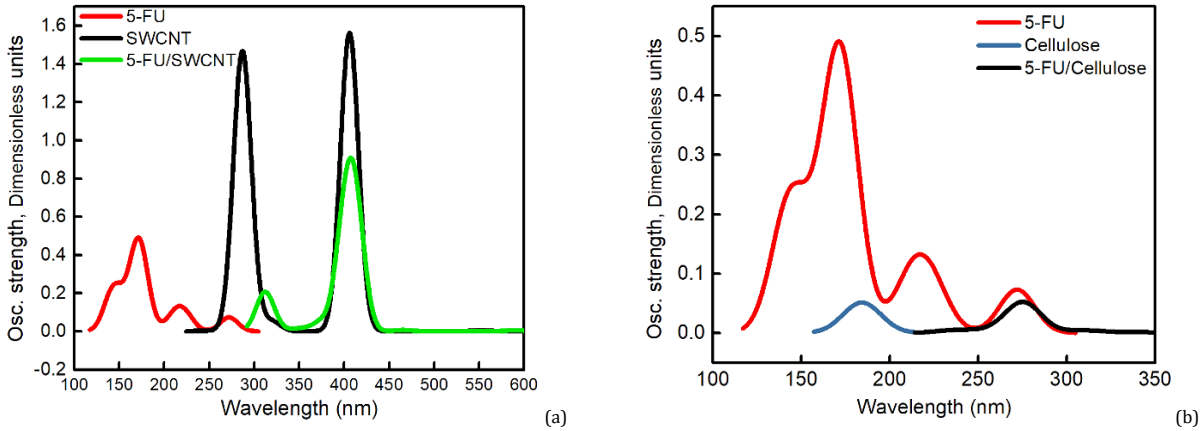

Figure 5. Optical spectra of the studied systems (a) the 5-FU/SWCNT complex and (b) the 5-FU/Cellulose complex compared to their isolated systems.

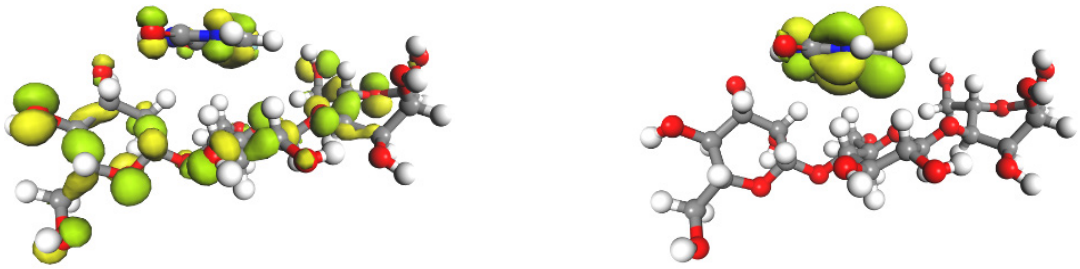

Figure 6. The overlapping behaviour of occupied orbitals of both drug and cellulose carrier of H-1 region.

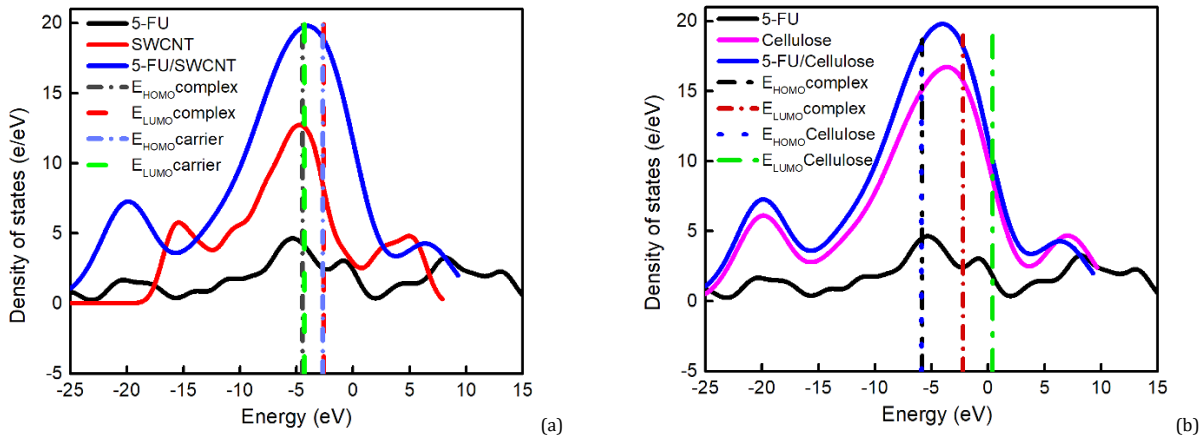

Figure 7. The density of states for (a) the 5-FU/SWCNT and (b) 5-FU/Cellulose complexes compared to their isolated systems. Vertical dashed lines indicate the HOMO and LUMO energy values.

This peak cannot be reproduced on a complex, who gives a maximum absorption at a wavelength of 276 nm due to a charge transfer from H−1 → L. From Figure 6, this clear difference can be attributed to the overlapping behavior of occupied orbitals of both drug and Cellulose carrier in H−1 orbital, and to the shift of the electron-accepting center from Cellulose equatorial hydroxyl groups to the 5-FU ring in LUMO orbitals. This overlapped behavior can evidently be observed at the fourth absorption peak of the 5-FU drug. The complexes show a good response to UV light in the wavelength range of 250-400 nm. This property can use to control the release of the drug using a "switch-on switch-off" mechanism and offers an insight towards phototherapy and skin photoprotection treatments [28].

3.5. Density of States (DOS)

Density of states analysis of the adsorption complexes, carriers and the isolated 5-FU drug in water media is shown in Figure 7. In general, the density of states does not show any HOMO and LUMO orbitals separation, indicating that the studied systems have a metallic character. The DOS shape of the 5-FU/Cellulose is very close to that of the pure Cellulose carrier, however, the relative intensity of the peaks passes to high value due to the significant increase of available states upon adsorption. This increase makes more states for electron occupation and facilities the charge transfer between the 5-FU drug and the cellulose carrier.

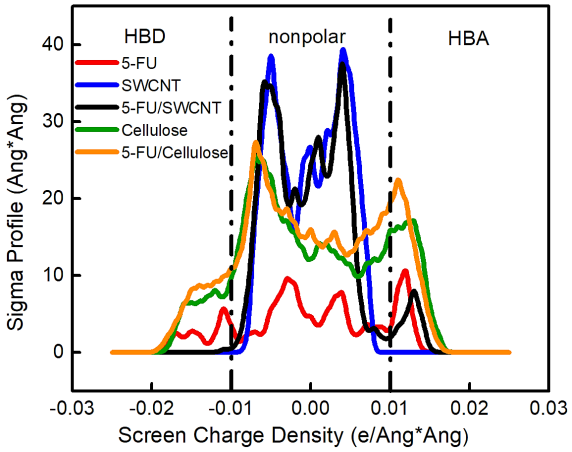

Figure 8. The COSMO sigma profile of 5-FU drug, SWCNT, cellulose, and their complexes.

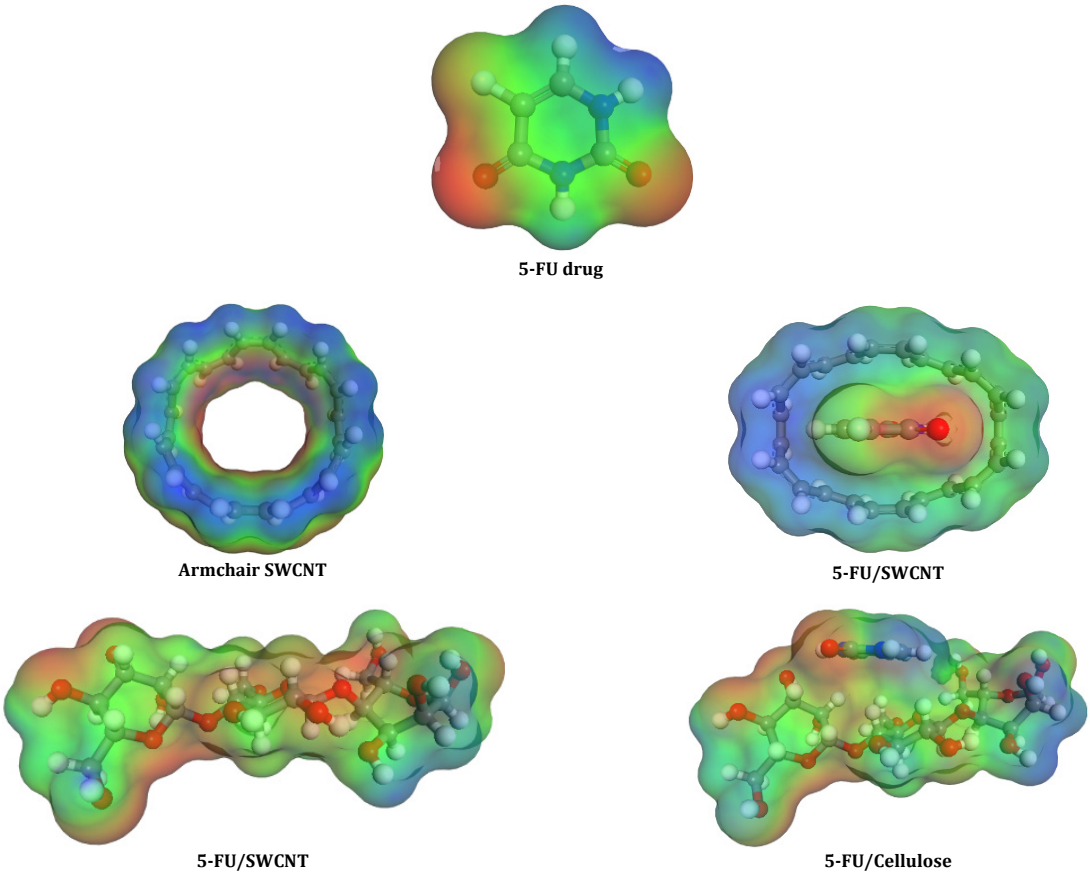

Figure 9. The COSMO surface for the 5-FU, SWCNT, cellulose and their complexes, respectively.

Similar behaviour is observed in the 5-FU/SWCNT complex; however, there is a shift in the peak positions of the complex in the areas far from HOMO LUMO orbitals.

3.6. COSMO study

In the solution medium, sigma profiles describe the nature of the compounds based on their affinity to interact with each other. Generally, there are two different regions that usually use to describe the molecular interaction, which are the hydrogen bonding and the nonpolar or hydrophobic region. The threshold values of the hydrogen bond interaction are usually taken from -0.01 to 0.01 e/Å^2 [29]. Any Compound possesses symmetrical peaks between this range interact via van der Waals forces. Whereas any compound possesses the value outside this range acts as a hydrogen bond acceptor (HBA) in a positive range and a hydrogen bonding donor (HBD) in a negative range of the sigma scale [30]. Figures 8 and 9 show the COSMO sigma profile and their surfaces of the 5-FU drug, pure carriers and their complexes implemented in DMol3 module.

As could be seen in Figure 8, the sigma profile of the 5-FU/SWCNT complex has the same symmetrical peaks as SWCNT in the nonpolar region. A developed COSMO peak in the positive range of the sigma scale means the complex has affinity toward HBA. The COSMO sigma profile peaks of the 5-FU/Cellulose and its components distributed significantly between and on either

side of the hydrogen bond threshold. That is, they can interact with each other either and with water via HBD or HBA. This interaction can be attributed to the presence of nitrogen and/or oxygen atoms, which are linked with or without hydrogen atoms, respectively. The peak intensity of a positive range is significantly looks higher than those peaks found in a negative range. This indicates that the complex has a better affinity toward HBA. In comparison with the 5-FU/Cellulose, the sigma profile peaks of the 5-FU/SWCNT complex reflect a hydrophobic effect of SWCNT carrier. The presence of the 5-FU drug on a carrier surface develops the affinity toward HBA both complexes, which enhances their solubility in biological systems. The 3D sigma surfaces of the solvation diagram represent the interaction regions by colored map in Figure 9. The extent of screening charge varies from -0.03 e/Å^2 (blue) to 0.03 e/Å^2 (red). Using Blue-green-red colored map, the molecular polarity can inversely be read on the sigma scale. The red part represents a positive COSMO charge density, which arises from negative molecular regions or hydrogen bond acceptor (HBA). The blue part represents a negative COSMO charge density arising from positive molecular regions or hydrogen bond donor (HBD). The yellow and green parts represent the nearly neutral charges of the molecular regions, which describe the hydrophobic behavior of the surface [2,29].

4. Conclusion

Herein, the adsorption behavior of the 5-FU anticancer drug on the surface of the SWCNT and the bio-fiber Cellulose was calculated by the DFT and MC simulation methods. Afterward, the frontier orbital energies, optical spectra, and density of states were analyzed in order to understand the mechanism of the interactions. The values of the adsorption energy indicate that the complexes are thermodynamically stable. The obvious difference of the HOMO → LUMO energies and the absorption peak position of the Cellulose complex indicate that the orbital configurations are changed. The complex became more reactive to add an electron to the LUMO level and more polarizable. The charge transfer centers completely shift to the carriers indicating a significant influence on their electronic structure. The electronic charge transfer happens in the interface of the electro-negatively centers of O3, N4, and N5 atoms of the 5-FU ring to the nearest atoms in the SWCNT tube by van der Waals forces. Whereas the N4 and H10 works as centers of interaction with a Cellulose carrier, in agreement with the formation of the H-bonding interactions. Based on COSMO model, the complex shows the affinity toward hydrogen bond acceptor, which enhances their solubility. These results imply that the carrier systems are more sensitive toward 5-fluorouracil adsorption and they can successfully be used as a drug delivery tool in biological systems.

Disclosure statement

Conflict of interest: The authors declare that they have no conflict of interest.
Ethical approval: All ethical guidelines have been adhered.
Sample availability: Samples of the compounds are available from the author.

ORCID and Email

Eshraq Ahmed Abdullah
ali123456yemen@gmail.com
https://orcid.org/0000-0001-9698-6203

References

[1]. Akkın, S.; Varan, G.; Bilensoy, E. A Review on Cancer Immunotherapy and Applications of Nanotechnology to Chemoimmunotherapy of Different Cancers. *Molecules* **2021**, *26* (11), 3382.
[2]. Bououden, W.; Benguerba, Y.; Darwish, A. S.; Attoui, A.; Lemaoui, T.; Balsamo, M.; Erto, A.; Alnashef, I. M. Surface Adsorption of Crizotinib on Carbon and Boron Nitride Nanotubes as Anti-Cancer Drug Carriers: COSMO-RS and DFT Molecular Insights. *J. Mol. Liq.* **2021**, *338* (116666), 116666.
[3]. Rodrigues, D.; de Souza, T.; Coyle, L.; Di Piazza, M.; Herpers, B.; Ferreira, S.; Zhang, M.; Vappiani, J.; Sévin, D. C.; Gabor, A.; Lynch, A.; Chung, S.-W.; Saez-Rodriguez, J.; Jennen, D. G. J.; Kleinjans, J. C. S.; de Kok, T. M. New Insights into the Mechanisms Underlying 5-Fluorouracil-Induced Intestinal Toxicity Based on Transcriptomic and Metabolomic Responses in Human Intestinal Organoids. *Arch. Toxicol.* **2021**, *95* (8), 2691–2718.
[4]. Safdari, F.; Raissi, H.; Shahabi, M.; Zaboli, M. DFT Calculations and Molecular Dynamics Simulation Study on the Adsorption of 5-Fluorouracil Anticancer Drug on Graphene Oxide Nanosheet as a Drug Delivery Vehicle. *J. Inorg. Organomet. Polym. Mater.* **2017**, *27* (3), 805–817.
[5]. Entezar-Almahdi, E.; Mohammadi-Samani, S.; Tayebi, L.; Farjadian, F. Recent Advances in Designing 5-Fluorouracil Delivery Systems: A Stepping Stone in the Safe Treatment of Colorectal Cancer. *Int. J. Nanomedicine* **2020**, *15*, 5445–5458.
[6]. Sethy, C.; Kundu, C. N. 5-Fluorouracil (5-FU) Resistance and the New Strategy to Enhance the Sensitivity against Cancer: Implication of DNA Repair Inhibition. *Biomed. Pharmacother.* **2021**, *137* (111285), 111285.
[7]. Patra, J. K.; Das, G.; Fraceto, L. F.; Campos, E. V. R.; Rodriguez-Torres, M. D. P.; Acosta-Torres, L. S.; Diaz-Torres, L. A.; Grillo, R.; Swamy, M. K.; Sharma, S.; Habtemariam, S.; Shin, H.-S. Nano Based Drug Delivery Systems: Recent Developments and Future Prospects. *J. Nanobiotechnology* **2018**, *16* (1), 71.
[8]. Freitas, C. M. P.; Coimbra, J. S. R.; Souza, V. G. L.; Sousa, R. C. S. Structure and Applications of Pectin in Food, Biomedical, and Pharmaceutical Industry: A Review. *Coatings* **2021**, *11* (8), 922.
[9]. Ravikumar, R.; Peng, M. M.; Abidov, A.; Babu, C. M.; Vinodh, R.; Palanichamy, M.; Choi, E. Y.; Jang, H.-T. Nanofibrous Polymers Blend of Fluorouracil Loaded Chitosan-Hydroxy Ethyl Cellulose/ Poly Vinyl Alcohol: Synthesis and Characterization. *Int. j. bio-sci. bio-technol.* **2016**, *8* (2), 295–306.
[10]. Yusefi, M.; Shameli, K.; Jahangirian, H.; Teow, S.-Y.; Umakoshi, H.; Saleh, B.; Rafiee-Moghaddam, R.; Webster, T. J. The Potential Anticancer Activity of 5-Fluorouracil Loaded in Cellulose Fibers Isolated from Rice Straw. *Int. J. Nanomedicine* **2020**, *15*, 5417–5432.
[11]. Khoshbayan, B.; Morsali, A.; Bozorgmehr, M. R.; Beyramabadi, S. A. Structural and Energetic Analysis of Cyclic Peptide-Gold Nano-Drug Delivery System: A DFT Study. *Nanosistemy fiz. him. mat.* **2021**, *12* (5), 612–622.
[12]. Kurban, M.; Muz, İ. Theoretical Investigation of the Adsorption Behaviors of Fluorouracil as an Anticancer Drug on Pristine and B-, Al, Ga-Doped C36 Nanotube. *J. Mol. Liq.* **2020**, *309* (113209), 113209.
[13]. Javan, M. B.; Soltani, A.; Azmoodeh, Z.; Abdolahi, N.; Gholami, N. A DFT Study on the Interaction between 5-Fluorouracil and B12N12 Nanocluster. *RSC Adv.* **2016**, *6* (106), 104513–104521.
[14]. Wazzan, N.; Soliman, K. A.; Halim, W. S. A. Theoretical Study of Gallium Nitride Nanocage as a Carrier for 5-Fluorouracil Anticancer Drug. *J. Mol. Model.* **2019**, *25* (9), 265.
[15]. Materials Studio package, BIOVIA, San Diego: Dassault Systèmes, USA, 2017, https://www.3ds.com/products-services/biovia/products/molecular-modeling-simulation/ (accessed Nov 23, 2021).
[16]. Abdalla, M. A. M.; Peng, H.; Wu, D.; Abusin, L.; Mbah, T. J. Prediction of Hydrophobic Reagent for Flotation Process Using Molecular Modeling. *ACS Omega* **2018**, *3* (6), 6483–6496.
[17]. Delley, B. An All-electron Numerical Method for Solving the Local Density Functional for Polyatomic Molecules. *J. Chem. Phys.* **1990**, *92* (1), 508–517.
[18]. Delley, B. From Molecules to Solids with the DMol3 Approach. *J. Chem. Phys.* **2000**, *113* (18), 7756–7764.
[19]. Ali, A. M.; Yahya, N.; Mijinyawa, A.; Kwaya, M. Y.; Sikiru, S. Molecular Simulation and Microtextural Characterization of Quartz Dissolution in Sodium Hydroxide. *J. Pet. Explor. Prod. Technol.* **2020**, *10* (7), 2669–2684.
[20]. Boraei, A. T. A.; Haukka, M.; Sarhan, A. A. M.; Soliman, S. M.; Barakat, A. Intramolecular Hydrogen Bond, Hirshfeld Analysis, AIM; DFT Studies of Pyran-2,4-Dione Derivatives. *Crystals (Basel)* **2021**, *11* (8), 896.
[21]. Grabowski, S. J. Chapter 1. Hydrogen Bond – Definitions, Criteria of Existence and Various Types. In *Theoretical and Computational Chemistry Series*; Royal Society of Chemistry: Cambridge, 2020.
[22]. Compañy, A. D.; Juan, A.; Brizuela, G.; Simonetti, S. 5-Fluorouracil Adsorption on Hydrated Silica: Density Functional Theory Based-Study. *Adsorption (Boston)* **2017**, *23* (2–3), 321–325.
[23]. Shojaie, F.; Dehghan, M. Theoretical Study of Functionalized Single-Walled Carbon Nanotube (5, 5) with Mitoxantrone Drug. *Nanomed. J.* **2016**, *3* (2), 115–126.
[24]. Khanmohammadi, A.; Mohammadi, M. Theoretical Study of Various Solvents Effect on 5-Fluorouracil-Vitamin B3 Complex Using Pcm Method. *J. Chil. Chem. Soc.* **2019**, *64* (1), 4337–4344.
[25]. Islam, M. J.; Kumer, A.; Sarker, N.; Paul, S.; Zannat, A. The Prediction and Theoretical Study for Chemical Reactivity, Thermophysical and

Biological Activity of Morpholinium Nitrate and Nitrite Ionic Liquid Crystals: A DFT Study. *Adv. J. Chem. A* **2019**, *2* (4), 316–326.
[26]. Mirali, M.; Jafariazar, Z.; Mirzaei, M. Loading Tacrine Alzheimer's Drug at the Carbon Nanotube: DFT Approach. *Lab-in-Silico* **2021**, *2* (1), 3–8.
[27]. Karachevtsev, V. A.; Plokhotnichenko, A. M.; Karachevtsev, M. V.; Leontiev, V. S. Decrease of Carbon Nanotube UV Light Absorption Induced by π–π-Stacking Interaction with Nucleotide Bases. *Carbon N. Y.* **2010**, *48* (13), 3682–3691.
[28]. Karisma, V. W.; Wu, W.; Lei, M.; Liu, H.; Nisar, M. F.; Lloyd, M. D.; Pourzand, C.; Zhong, J. L. UVA-Triggered Drug Release and Photo-Protection of Skin. *Front. Cell Dev. Biol.* **2021**, *9*, 598717.
[29]. Klamt, A.; Eckert, F. COSMO-RS: A Novel and Efficient Method for the a Priori Prediction of Thermophysical Data of Liquids. *Fluid Phase Equilib.* **2000**, *172* (1), 43–72.
[30]. Suhaimi, H. E.; Hizaddin, H. F.; Wazeer, I.; El Blidi, L.; Hashim, M. A.; Hadj-Kali, M. K. Simultaneous Extraction of Sulfur and Nitrogen Compounds from Model Diesel Fuel Using Neoteric Green Solvents. *ACS Omega* **2021**, *6* (34), 22317–22332.